Preferred citation: A. Mattsson and T. Uesaka. Time-dependent, statistical failure of paperboard in compression. In **Advances in Pulp and Paper Research, Cambridge 2013**, *Trans. of the XVth Fund. Res. Symp. Cambridge, 2013*, (S.J. I'Anson, ed.), pp 711–734, FRC, Manchester, 2018. DOI: 10.15376/frc.2013.2.711.

TIME-DEPENDENT, STATISTICAL FAILURE OF PAPERBOARD IN COMPRESSION

Amanda Mattsson and Tetsu Uesaka

Mid Sweden University, FSCN, Sundsvall, Sweden amanda.mattsson@miun.se and tetsu.uesaka@miun.se

ABSTRACT

This paper concerns the question of how to predict mechanical performance of box and paperboard subjected to fluctuating load/environmental conditions encountered in end-use. Particularly such performance is notoriously variable (stochastic), and is known to be very difficult to predict.

We have developed a theoretical framework for treating time-dependent, statistical failure based on the recent progresses in statistical physics of disordered materials. The main objective of this study is to experimentally determine the three key parameters that fully characterise the failure of component board subjected to general loading histories, namely the parameter c related to static strength and its uniformity, the load sensitivity/durability parameter ρ, and the uniformity parameter β of creep lifetime. Results showed that creep lifetime distribution is highly skewed with extreme scatters, but the distribution is still a class of Weibull distribution and can be handled without any problem. The durability parameter ρ also showed high values comparable with those for fibre-composites. These two results explained very well the variability and load sensitivity of box creep performance observed in the literature.

This proposed approach offers a new set of material property parameters, other than traditional strength, that can be fully exploited in both materials and structural design to enhance end-use performance in the most resource-efficient manner.

INTRODUCTION

Lifetime is probably the most important performance parameter of container box, which is normally subjected to varying load and humidity/temperature conditions in end-use. However, it is also the most difficult parameter to measure and predict. Much attention, therefore, has been drawn to determine static strength (or fast fracture strength) instead of lifetime. (A historical review of corrugated compression strength can be found in [38–39].)

There are significant differences between strength test conditions and end-use conditions. In laboratory testing, *strength* is measured either at a constant displacement rate or at a constant force rate. In end-use, on the other hand, board and box are subjected to a much more complicated loading history, such as shown in Fig. 1. Important differences between strength measured in laboratory and actual mechanical performance in end-use are (1) load level, (2) time scale, (3) environment, and (4) variability. Generally, service load in end-use is much lower than ultimate strength, except occasional peak loads (Fig. 1). Second, as related to the applied load level, the time scale is days, weeks and months in end-use, as opposed to only seconds and minutes in laboratory testing. Third, temperature and humidity always vary in end-use, whereas they are typically kept constant in laboratory. Accordingly, a question has been posed, among packaging professionals, on whether strength parameters, such as BCT (box compression test), SCT (short span compression test), RCT (ring crush test), etc., really represent real end-use performance. In fact, there have been already some evidences accumulated in the fields: stronger board does not necessarily perform better in the long term response (for example, [40]). As an alternative, creep tests have been performed on boxes and component boards under constant or varying humidity conditions, and have been analysed in various research laboratories. (A recent review of the creep deformation and creep failure can be found in [1].) Although substantial work has been done to investigate creep deformation

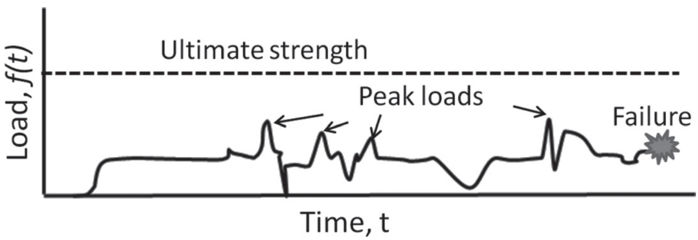

Figure 1. Schematic of load history in end-use.

behaviour, lifetime measurements were surprisingly scarce [1–8]. This may be related to the last point, variability. Failure in end-use is of stochastic nature, that is, it happens in a very unpredictable manner. It was recognised in the early literature [41] that creep lifetime of boxes normally exhibits enormous statistical variations. For example, the values of the coefficient of variation (COV) of creep lifetime of boxes were estimated from various data in the literature [10], and showed 70% to 90%. It should be noted that these values were obtained under nominally same environmental conditions, and, therefore, in end use, the variability would be even greater. This uncertainty of lifetime might have plagued many researchers and board manufacturers in tackling this problem, and eventually have drawn their attention to more tractable tests, i.e., creep deformation tests and eventually static strength tests. The basic motivation of performing creep deformation tests, instead of creep failure, is based on the fact that the rate of creep deformation (particularly the secondary creep rate) is almost inversely proportional to the secondary creep rate, as found in Monkman and Grant in 1950s [37]. In essence, the higher the creep rate, the shorter the lifetime. Using this empirical equation, together with other assumptions related to box strength, Coffin developed a model to predict creep lifetime distribution from box strength distribution [1].

However, the fundamental questions still remain:

- Does strength represent real performance of box and board subjected to a general loading condition, such as shown in Fig. 1? If not, what should we evaluate?
- How to deal with enormous variability of lifetime? What is causing this? Box structures, converting defects, board structures, or fibres?
- Facing these challenges, how to design box and component boards to enhance real end-use performance?

This paper is a formal attempt to answer the above questions by using non-empirical approach based on the recent progresses in statistical physics of failure of disordered materials. The model directly deals with a general loading mode, such as in Fig. 1, so that we can discuss the distributions of strength, stretch and lifetime for linear loading, creep, fatigue, and random loading in a unified way. We will first apply the model, which was proposed earlier [9, 10], to component boards, instead of boxes, since the latter requires an additional formulation of structural mechanics. The main objective of this paper is to experimentally determine the three key material parameters that characterise time-dependent, statistical failure. These three characteristic parameters are defined in the theoretical background section.

THEORETICAL BACKGROUND

The fact that strength varies statistically is well recognised from the very early days of fibre and textile research (for example, [42]). Using the weakest-link hypothesis and *a priori* distribution of the element strength of fibre/yarn, the early researchers were able to analytically calculate the strength distribution as well as the size dependence of strength, another important aspect of strength. This classical approach was later expanded and applied to other non-fibre materials, and a large number of strength data were organised by, what is known today, Weibull distribution [43]. Although, so called, Weibull statistics is extremely popular in materials science and experimental mechanics areas, the estimated (Weibull) parameters have very little connection with physics behind, and are phenomenological, curve-fitting parameters.

Almost independently from the above work, statistical failure has been studied intensively in statistical physics, using lattice models, fibre bundle models, cellular automata, and molecular dynamics, with close interactions with fracture mechanics and extreme-value statistics. Time-dependency of statistical failure was first formulated by Coleman with a rigorous mathematical framework [11–14]. Subsequently, it has become almost a default model for investigating dynamic failure of disordered materials in statistical physics. This paper also uses his formulation as a starting model for *fibre*. However, we will demonstrate that it can be utilised, with very little change, on a fibre network level as well. Most importantly, the parameters that Coleman defined can be easily determined experimentally.

Single fibre model

Paper and board possess a highly disordered, fibre network structure. As it is loaded, there are always basic structural elements that carry the load. We first define the element in the fibre network, called "fibre", by following Coleman's terminology [11–14]. The fibre doesn't have to be actual papermaking fibres, but is a basic structural unit (or fictitious element) that controls the micro-processes of compression failure of fibre network. As load and environmental stimuli (temperature and humidity) are applied, fibres gradually break down (or are damaged). Generally, the damage evolution (breakdown rule) is expressed as:

$$\frac{d\Omega}{dt} = \phi\left[f, \frac{df}{dt}, \frac{d^2f}{dt^2}, \dots, \Omega, m, \frac{dm}{dt}, \frac{d^2m}{dt^2}, \dots\right] \tag{1}$$

where Ω is a damage parameter, f(t) ($t \geq 0$) is load history, and m(t) is moisture or, generally, environmental history. The above equation is not a meaningless generalisation of what is already known. In fact, higher degree of the derivatives are included to express a more general dissipation process, such as seen in the generalised Maxwell model in viscoelasticity. Therefore, this general breakdown rule can include fatigue, ageing, and even self-healing type phenomena. From the context of fibre-based materials, it can, of course, also include the effects of accelerated creep [15–19]. When the damage evolution rate is a sole function of load (i.e., constant environment), the most accepted form in statistical physics (and analytically most convenient form) is:

$$\frac{d\Omega}{dt} \propto f^{\rho} \tag{2}$$

where ρ is load sensitivity parameter, i.e., as ρ increases, the damage evolution accelerates. (Another form, which is often used in polymer physics/chemistry, is the exponential form. This form gives a linear relation between logarithm of average creep lifetime and load. Phoenix and Tierney showed that, unlike general belief, the power law form in Eq. (2) is much better approximation of the activation potential function than the exponential form [28].) The damage at time t can be obtained by integrating Eq. (2) for an entire load history that is magnified by the exponent ρ. The probability that fibres fail before time t depends on the damage accumulated up to time t. The greater the damages, the higher the failure probability. Coleman used an extreme-value argument to obtain the cumulative distribution function F of lifetime, t_B:

$$F(t_B) = 1 - exp\{-b\Omega(t_B)^{\beta}\} \tag{3}$$

where β is a mathematical parameter, related to the lower tail distribution of damages (micro/nano-pores and cracks) in materials, and b is a constant related to damage growth. Combining Eqs. (2) and (3), we can obtain the cumulative distribution function of lifetime when a fibre is subjected to a general loading history f(t) ($t \geq 0$):

$$F(t_B) = 1 - exp\left\{-c\left[\int_0^{t_B} f(t)^{\rho}\, dt\right]^{\beta}\right\} \tag{4}$$

where c absorbs all constants. Equation (4) is a general form of lifetime distribution when load *fluctuates* as a function of time, such as shown in Fig. 1. Therefore, the above equation is the most general expression for lifetime of fibre subjected to *any* loading history (e.g. creep, linear loading, cyclic loading, and random loading). In the equation, there are three important material parameters: c, ρ, and β. As we will show later, these parameters represent multi-facet nature of mechanical performance in end-use, and can be determined experimentally by a series of creep tests. (Note that creep test is not the only test for determining these parameters.) Once determined, one can predict lifetime of fibre for any loading histories.

In the case of creep loading ($f(t)=f_0$, constant), Equation (4) becomes:

$$F(t_B) = 1 - exp\{-cf_0^{\rho\beta} t_B^{\beta}\} \tag{5}$$

The implications of this equation are, first, that creep lifetime distribution of "fibre" is Weibull distribution. The exponent β is related to the uniformity of creep lifetime distribution, since it is a unique function of the coefficient of variation (See Appendix). The higher the value of β, the sharper the creep lifetime distribution. In other words, β is a factor representing long-term reliability. For other parameters, we can find their physical meanings by obtaining the basic statistical quantities from Eq. (5). Average lifetime $E\{t_B\}$, median lifetime t_m, and the coefficient of variation COV are determined from Eq. (5) as follows:

$$E\{t_B\} = c^{-\frac{1}{\beta}}\Gamma\left(1+\frac{1}{\beta}\right) f_0^{-\rho} \tag{6}$$

$$t_m = c^{-\frac{1}{\beta}} ln\,(2)^{\frac{1}{\beta}} f_0^{-\rho} \tag{7}$$

$$COV = \left[\frac{\Gamma(1+\frac{2}{\beta})}{\Gamma^2(1+\frac{1}{\beta})} - 1\right]^{1/2} \tag{8}$$

where Γ is gamma function. By taking logarithm of Eqs. (6) or (7), we obtain

$$log(E\{t_B\}) = log\left(c^{-\frac{1}{\beta}}\Gamma\left(1+\frac{1}{\beta}\right)\right) - \rho \cdot log(f_0) \tag{9}$$

Obviously, as we increase load f_0 in Eq. (9), average lifetime decreases. In order to derive a physical meaning of ρ, we denote the load that gives average lifetime $E\{t_B\}=1$ (sec.) as $f_{0,B}$. That is, the load $f_{0,B}$ represents a kind of short-term strength. Then, Equation (9) is converted into the following equation.

$$log(E\{t_B\}) = \rho \cdot log\left(\frac{f_{0,B}}{f_0}\right), \text{ or}$$

$$E\{t_B\} = \left(\frac{f_{0,B}}{f_0}\right)^{\rho} \tag{10}$$

Equation (10) shows that when comparing two materials (fibres) of the same short-term strength at the same applied load, the material with higher ρ gives longer lifetime. In other words, the parameter ρ represents durability or endurance of the material.

Another important implication of this model can be extracted from Eq. (8): The coefficient of variation of creep lifetime is *independent* of load. This means that, since average creep lifetime increases with decreasing load, the standard deviation of creep lifetime also increases with decreasing load. At this moment, there is no experimental data (for fibre) that will validate or invalidate this prediction.

The response to normal tensile and compression loading can also be derived from Eq. (4). In the case of tensile/compression tests at a constant loading rate α, strength f* is expressed as $\alpha \cdot t_B$. Therefore, from Eq. (4), we can obtain cumulative distribution of strength f* as follows:

$$G(f^*) = 1 - exp\left\{-\frac{c}{(\rho+1)^{\beta}\alpha^{\beta}}(f^*)^{\beta(\rho+1)}\right\} \tag{11}$$

Again, strength distribution of fibre is Weibull distribution. An important difference from the case of creep lifetime distribution is that the exponent for strength is $\beta(\rho+1)$, which is different from that for creep lifetime β. In other words, the variability of strength could be very different from that of creep lifetime, or vice versa, depending on the magnitude of ρ, the load sensitivity or durability parameter. As we will see later in the experimental data, this is indeed the case for linerboard samples.

Lastly, a physical interpretation of the parameter c can be obtained from Eq. (7) in a similar way to the parameter ρ. First we denote the load that will give the median creep lifetime t_m=1 (sec.) as $f_{0,max}$. This load, $f_{0,max}$, can be regarded as another measure of short-term strength expressed as median. Employing Eq. (7), we find

$$1 = c^{-\frac{1}{\beta}} ln\,(2)^{\frac{1}{\beta}} f_{0,max}^{-\rho}, \text{ or}$$
$$\mathbf{c} = \log(2) \cdot \mathbf{f}_{0,max}^{-\beta\rho} \sim \log(2) \cdot \mathbf{f}_{0,max}^{-\beta(\rho+1)} \qquad for\ \rho \gg 1 \tag{12}$$

As seen in the last expression in Eq. (12), c is related to short-term strength $f_{0,max}$, and its uniformity parameter $\beta(\rho+1)$: The higher the short-term strength and the higher the uniformity, the lower the parameter c.

In summary these three parameters c, ρ and β completely determine lifetime distribution for *any* loading histories through Eq. (4). The parameter c represents short-term behaviour related to average (median) strength and its uniformity. The parameters ρ and β both represent long-term behaviour related to durability and variability, respectively.

Fibre network model

The previous discussion concerns the failure of a single fibre element. In the case of fibre network, the failure of single fibre doesn't necessarily lead to failure of an entire system, unlike the case of single fibre or yarn. Instead, one fibre failure results in a transfer of the load of the failed fibre to another intact fibre(s). This load transfer or load sharing depends on how fibres are connected to each other in the fibre network. Failure of some fibres in the network creates a new state of load distribution in the fibre network, and, depending on the locations of failed fibres and their connections to other fibres, the propagations of failed sites vary and thus time-to-failure (lifetime) also varies. This is the central theme of the mechanics of statistical failure of disordered materials. There have been extensive studies in statistical physics area to determine the distributions of static strength and time-dependent strength (lifetime) using various structural models, such as lattice models and fibre-bundle models (FBM) with various modifications [20–29]. In this study we used FBM, because it is considered to be the best paradigm for capturing universal features of statistical mechanics of fibre network. It is also numerically still tractable to handle a very large system size that is more relevant to reality.

In FBM, fibres are aligned in parallel and share the same load in the beginning. As soon as one fibre fails, the load of the failed fibre is shared by the neighbouring fibre(s), so called local load sharing. As this failure process continues, a number of clusters, large and small, of fibre failure develop, and at some point the largest cluster triggers avalanches of the failure of remaining fibres, leading to entire system failure. Although the model appears (deceivingly) simple, no analytical solution has been obtained for the shape of distribution function, and for the relations with the key characteristic parameters of fibre, as we discussed in the previous section. Therefore, we performed numerical experiments to determine creep lifetime distributions of fibre bundle network as a function of system size (the number of fibres in the bundle), and fibre parameters (β and ρ) [10]. The most important result is that, as the system size grows and exceeds a certain threshold number, the distribution function of the system, $F_N(t_B)$ starts showing, so called, the weakest link scaling:

$$\mathbf{1 - F_N(t_B) = (1 - F_0(t_B; \rho, \beta))^N \approx exp\{-NF_0(t_B; \rho, \beta)\}} \tag{13}$$

or equivalently,

$$\mathbf{log\big(-log(1 - F_N(t_B))\big) = log(N) + log(F_0(t_B; \rho, \beta))} \tag{14}$$

where $F_0(t_B; \rho, \beta)$ is the characteristic distribution function, and N is the system size (the number of fibres). Equation (14) shows that, if the weakest-link scaling appears with increasing N, the system size effect is represented by a simple vertical shift log(N) of the curves. In our earlier study [30], we found that a typical system size when the weakest-link scaling appears was about 1.5–2.0 cm for 45g/m^2 sheets, about 10 times of a typical fibre length.

The rate of approaching to this scaling behaviour depends on load sensitivity parameter ρ: with increasing ρ, the rate increases. Figure 2 shows an example of such system size effect in the case of β=1 and ρ=10. In this study, we assumed a relatively high value of ρ as compared with the values from our previous study. This is because we found that experimental data for ρ obtained in this study were much higher than what we originally expected. It is clear that as the system size N increases, the curves quickly collapse to a single curve, which is later called "characteristic distribution function". In this example, the limiting shape is obtained already for N=5. An interesting observation is that the characteristic distribution of the fibre bundles is closer to the one for a single fibre when higher ρ is assumed. In other words, for those fibre networks with high ρ, the network response may be affected more by fibre properties rather than network structures.

The result of size scaling is extremely encouraging, because we can utilse this scaling result (Eq. (13)) to calculate the size effect of lifetime for real specimens. (However, the size effect is generally logarithmic (log(N)), so that the effect is not extremely strong.)

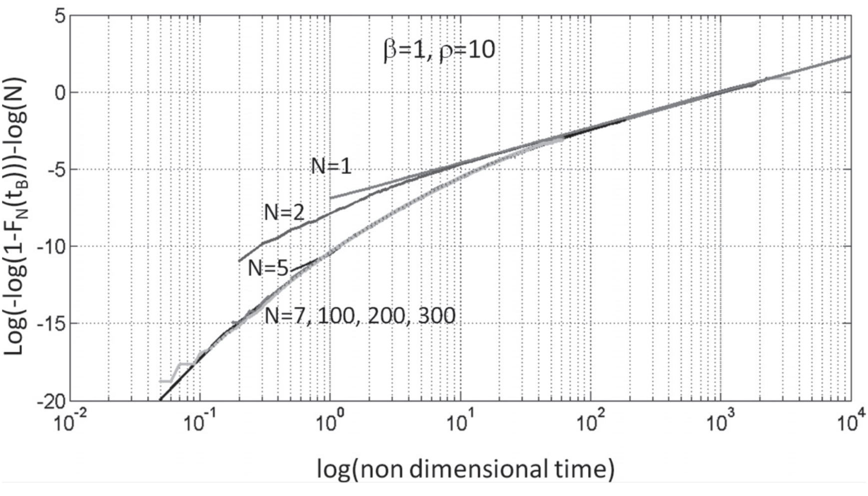

Figure 2. Weibull plots of cumulative distribution function of fibre bundles for different system sizes. In this plot the base 10 was used for logarithm. (The subsequent figures are expressed with natural logarithm.)

It should also be noted that the collapsed curve is not linear. This means that the cumulative distribution of a large fibre bundle system is *not* Weibull distribution (See also Appendix). However, as Phoenix and Tierney also indicated [28–29], within the range of probability that normal experiments can access (e.g., in this study, $0.01<F_N(t_B)<0.99$, the corresponding width in the y-axis is 2.66, an approximately half of the minor tick interval), one can hardly see the curvature, and the collapsed curve can be seen as linear. Using this piecewise linear approximation, we can express the cumulative distribution function of a fibre-bundle system, again, by Weibull distribution:

$$F_N(t_B) = 1 - exp\{-c_N f_0^{\rho\beta_N} t_B^{\beta_N}\} \tag{15}$$

where c_N and β_N generally depend on the system size. This result confirms many observations from empirical curve-fitting that Weibull distribution hardly breaks down within the experimental probability range. This ubiquitous (and fortuitous) nature of Weibull distribution is due to the above special asymptotic property of the underlying distribution, and also due to the robustness of the algebraic form of its kernel distribution ($F_0(t_B)$). It should also be noted that the load scaling (f_0^ρ) in Eq. (15) is the same as that of fibre in Eq. (5). The implication of these results to experimental analyses is important: one can utilise all relationships originally developed by Coleman for single fibre also for fibre bundle systems. Fibre bundle can be further connected in a series to create a chain of fibre bundles (Fig. 3), in

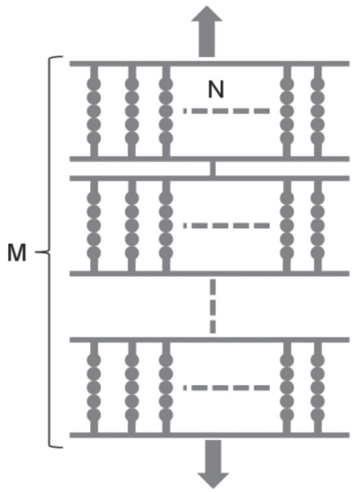

Figure 3. A chain of fibre bundle model. N: the number of fibres, and M: the number of fibre bundles.

order to mimic fibre network. In this case, all the relationships derived are maintained, except that N is simply replaced with MN, where M is the number of fibre bundles (Fig. 3). A still outstanding question may be whether such chain of fibre bundle model represents time-dependent, statistical failure of actual fibre network. This is still an open question, but numerical simulations performed in lattice networks so far showed, at least qualitatively, a close resemblance to those general predictions from fibre bundle models [31].

Based on these theoretical preparations, we will determine the three key parameters for a fibre network system, i.e., linerboard. (In the following we will suppress the dependence on the system size in the notation of these parameters. However, it should be understood that they are generally dependent on the sample size.)

EXPERIMENTS

In order to determine the key parameters that control the distributions of time-dependent, statistical failure (Eq. (4)), a series of creep failure tests are performed on linerboards using a long-span creep compression tester at SCA R&D Centre in Sundsvall, Sweden. The equipment was constructed by Jarmo Tulonen at TJT-Teknik AB, which is based on the concept developed at Innventia (former STFI). An overview of the creep equipment is shown in Fig. 4.

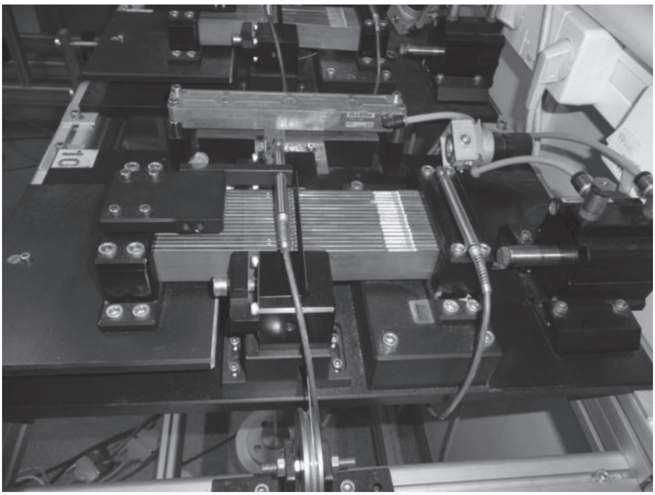

Figure 4. Overview of the creep equipment. The sample is placed between the two set of staples which support the sample to prevent buckling in compression.

The areas of the samples that are loaded in the tester are 25×61 mm, where the compression load is applied in the CD. Prior to creep tests, a series of constant strain-rate tests were performed to determine edgewise compressive strength. These compressive strength tests were done in order to apply proper levels of load for the creep tests. Approximately 50–100 strips were tested at a given creep load to determine the distribution functions of lifetime. The distribution function was determined by sorting the values of lifetime in ascending order and assigning the probability of i/n for the i-th lifetime value, where n is the total number of samples tested. For those samples that failed instantly or didn't fail within the set time, we only used the probability values of the remaining samples for the data analyses. For example, suppose three samples failed instantly, we assigned the probability of 4/n for the 4th sample, 5/n for the 5th sample, so forth. In order to represent the average lifetime, we used median instead of the standard average. This is because the values of normal average are sensitive to the presence or lack of extreme high/low tails in the case of lifetime distributions, whereas median values are more stable and robust.

The samples that are tested are a bleached kraft liner and an unbleached test liner with a grammage of 135g/m^2.

RESULTS AND DISCUSSION

Lifetime distribution and estimation of uniformity parameter β

Figure 5 shows typical creep deformation curves, and corresponding failure events for a kraft liner tested at the same applied load. As seen in the figure, the failure events tend to occur almost in a random fashion. It is difficult to find specific time range where the failure takes place. It is also interesting to note that for those samples which failed earlier, the corresponding creep deformation rates tended to be greater. (We will later discuss more details.)

In order to quantify the lifetime distributions, we plotted the cumulative distributions of creep lifetime in the Weibull format in Figures 6 and 7. As explained in Appendix, this plotting format is the most critical test to examine whether the distribution follows Weibull distribution or not.

It can be seen that the plots are approximately linear, suggesting Weibull distribution. When forcing the linear fit of the data, the slopes of these plots (Weibull exponent) were 0.43–0.50. These values are extremely small as compared with those of tensile (or compressive) strength of paper, which is around 10–25 [32]. This big difference in Weibull exponent between lifetime and compression strength distributions can be explained by comparing Eq. (5) with Eq. (11). The Weibull exponent (the uniformity parameter) for lifetime distribution is β, while the same exponent for strength distribution is $\beta(\rho+1)$. Therefore, depending on

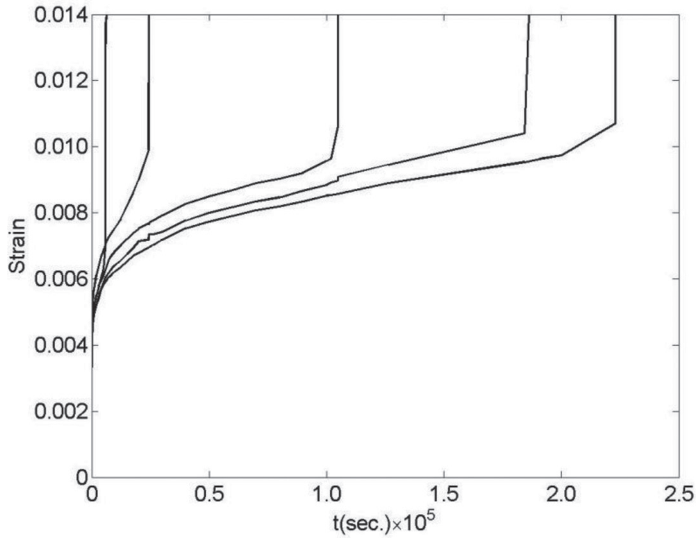

Figure 5. Typical creep curves for a bleached kraft liner applied to the same load.

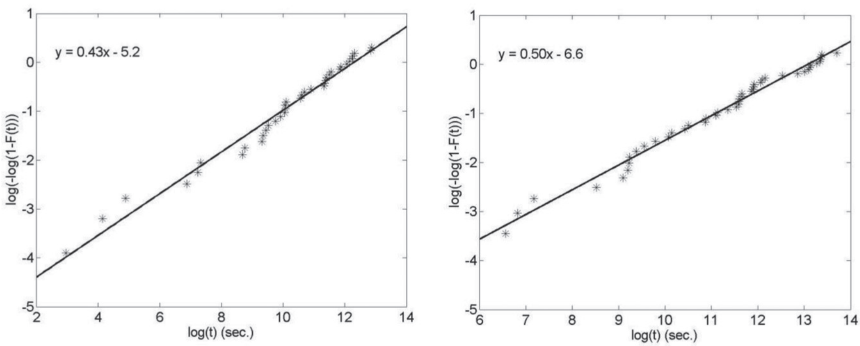

Figure 6 and 7. Lifetime distribution for a bleached kraft liner (left) and an unbleached test liner (right). The load level is about 80 percent of the compression strength of each sample in the CD.

the value of load sensitivity parameter ρ, these two distributions become considerably different. Particularly when ρ>>1 (we will show that this is the case in the next section), the lifetime distribution becomes extremely wide as compared with strength distribution. This difference in Weibull exponent is directly translated into the difference in the coefficient of variation (COV), since these two are uniquely related, as seen in Eq. (8) (See also Appendix). For example, we measured COV from the standard compression strength, which varied between 2.8–7.0% (10 data points), whereas the value of COV for creep lifetime varied between 224–279% (100 data points).

It may also be interesting to compare these COV values for linerboard with those for boxes. The COV values of creep lifetime for boxes were 70–90% [10], whereas the COV for linerboards were more than 200%! In other words, the large variability of creep lifetime of boxes may originate from the corresponding variability of the component boards.

This uncertainty of lifetime obviously makes the design of board properties and box structures extremely difficult. It may also temp box designers to overdesign box/board strength by using higher safety factor.

In order to obtain an intuitive picture of the shape of the distribution functions for lifetime and strength, cumulative distribution functions (CDF, left)) with raw data and their corresponding probability density functions (PDF, right) are plotted in Figure 8.

As can be seen, the distribution of lifetime is highly skewed, whereas strength distribution is more symmetric and closer to Gaussian distribution. The sharp rise in the cumulative distribution function (CDF) of lifetime is reflected in its probability density function (its differential). It should be noted that both lifetime and strength distributions are approximated by Weibull distribution, but with vastly different exponents. In other words, Weibull distribution is robust enough to handle very skewed distributions as well as normal distributions.

Figure 9 shows the β values estimated for different loads for the two different linerboards. There was no systematic change in β within the experimental range tested. This is also the basic requirement of Eq. (4).

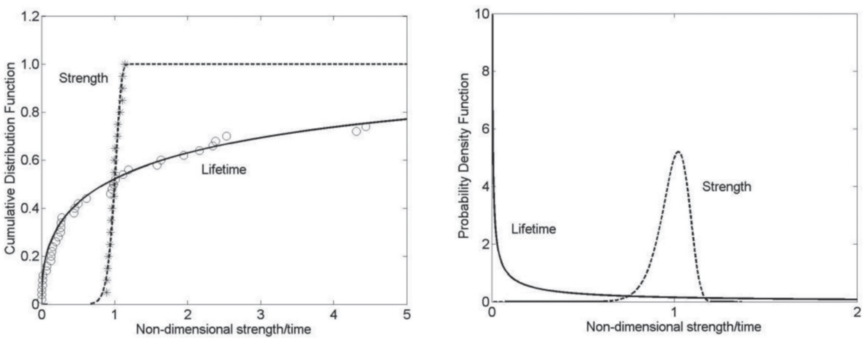

Figure 8. Cumulative distribution functions (left) and probability density functions (right) for lifetime and strength. The data are from bleached kraft liner at an 80% load of its compressive strength. The solid and dotted lines are fitted curves by Weibull distribution.

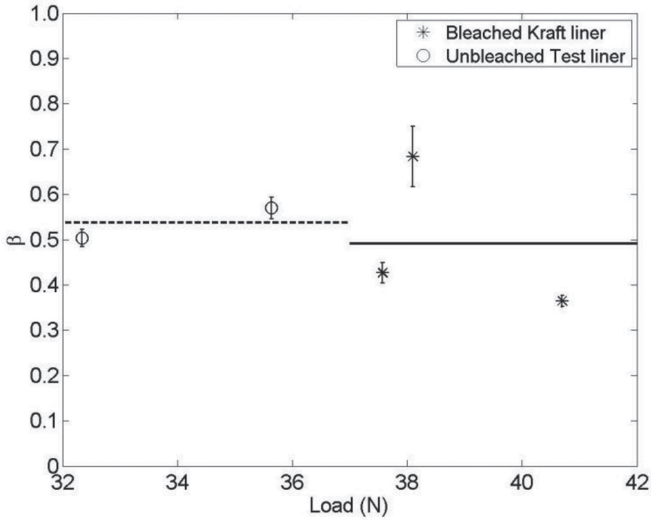

Figure 9. Uniformity parameter β estimated at different loads. The bar at each point represents 95% confidence interval.

Considering the fact that, in end-use, the lower tail of the time to failure is more important than its average, one need to focus more on this uniformity parameter β.

The estimation of load sensitivity parameter ρ

Load sensitivity parameter (ρ) determines the acceleration of the damage evolution (Eq. (2)). As ρ increases, the damage evolution accelerates and thus the failure probability increases. It also represents durability when compared at the same strength (Eq. (10)). Figure 10 shows the relationship between median lifetime and applied load for two different linerboards. Each data point represents a median value of 50–100 data points. Because of long-term testing, further data at lower load levels are still being collected.

As seen in Eq. (7), taking logarithm of both sides of Eq. (7) gives a linear relationship between log(median lifetime) and log(load), yielding the slope -ρ. The ρ values obtained for these boards were 47.7 for unbleached test liner and 53.5 for bleached kraft liner. These values are much higher than those estimated from Nyman's data [6] for corrugated *boxes*, varying between 1.7 and 14. They are also higher than those estimated from the data by Morgan [5], Stott [33], and Moody [4], ranging from 13 to 27 for corrugated boxes and 3 to 7 for corrugated

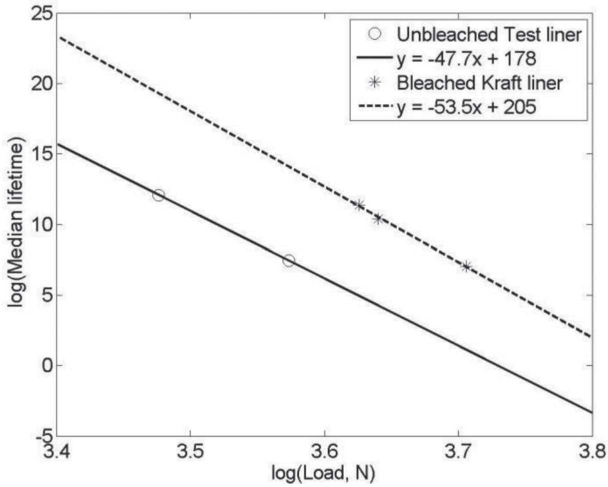

Figure 10. Median lifetime against load for two different linerboards. The median values at the load level 80%, 85% and 90% of maximum load are plotted. The number of data presented is about 50 samples for 80%, 50 samples for 85% load and 100 samples for 90% load.

panels. Again the very high load sensitivity of linerboard is an underlying factor for the high load sensitivity of boxes.

It is interesting to note that these values are comparable with those reported by Phoenix for Kevlar-Epoxy, Graphite fibre-epoxy, and S-glass fibre-epoxy composites [26]. At this stage it is not known what controls load sensitivity parameter in the context of pulping, papermaking and box manufacturing.

Fellers and co-workers also made a similar plot (log-linear plot, instead of log-log plot, of average lifetime vs. load) to compare tensile and compression creep failure [34]. They reported higher slope for compression, implying higher load sensitivity parameter for compression creep failure.

In Fig. 11 we re-plotted the previous data against load ratio (creep load divided by average compression strength in load unit). It is interesting to see that both two linerboards yielded a single line. This type of plotting is often attempted in order to collapse the data from different sources of board and box, but the degree of success varied. A question is whether the relation, such as seen in this figure, is universal among different samples or accidental. This question may be answered by rewriting the expression of median lifetime as a function of average compression strength through the use of Eqs. (6), (7) and (11):

$$t_m = \ln(2)^{\frac{1}{\beta}} \cdot c^{-\frac{1}{\beta(\rho+1)}} \cdot (\rho+1)^{-\frac{\rho}{(\rho+1)}} \cdot \alpha^{-\frac{\rho}{(\rho+1)}} \cdot \Gamma\left(1 + \frac{1}{\beta(\rho+1)}\right)^{-\rho} \cdot \left(\frac{f_0}{\langle f^* \rangle}\right)^{-\rho} \quad (16)$$

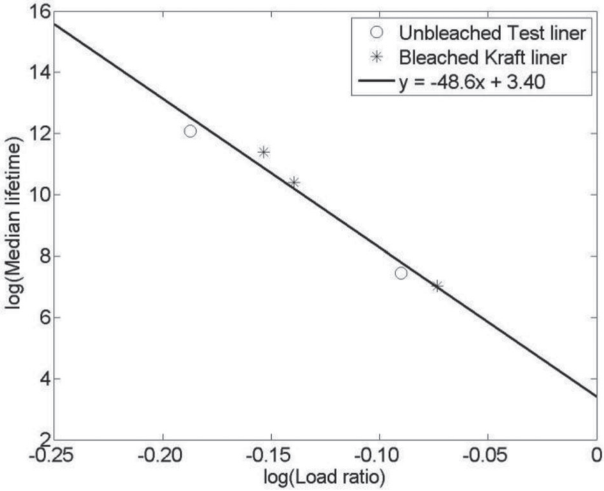

Figure 11. Median lifetime against load ratio (creep load/the average ultimate load in compression) for three different load levels and two different linerboards.

where <f*> is average compression strength. Inspecting the right-hand side of the above equation reveals that, if $\beta(\rho+1)$ is large in the order of 10–20 and both ρ and β are similar among the samples tested, then the log-log relationship of median lifetime and load ratio gives an approximately single collapsed line for different samples. (Note that the second term in the right-hand side of the equation includes [EQN??] expression, in which a large n value depresses any change in x.) Therefore, the relation obtained in Fig. (11) is not universal.

Dependence of creep lifetime on secondary creep rate

It is well known that creep deformation, particularly secondary creep rate, is an indication of final creep failure of corrugated box and board [3–4, 8, 35–36]. Secondary creep rate is defined as the slope of the linear part of the curves in Fig. 5. The most commonly used relation for describing lifetime and secondary creep rate is the following Monkman-Grant equation [37], which is an empirical equation found for creep failure in metals:

$$t_B = A \frac{d\varepsilon}{dt}^{-n} \tag{17}$$

where t_B is the lifetime, $d\varepsilon/dt$ the secondary creep rate, A is a constant, called “ductility factor”, and the exponent n is usually in the order of 1.

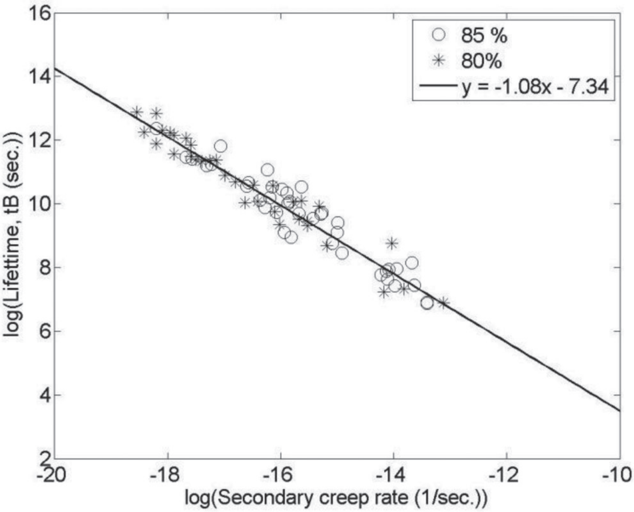

Figure 12. Lifetime against secondary creep rate for a bleached kraft liner on a load level of 80% (*) and 85% (circle).

In Fig. 12, we have also plotted individual data of lifetime and secondary creep for two different load levels from bleached kraft liner. As seen in the figure, Monkman-Grant empirical relation fits very well the data set, giving the value of exponent n approximately unity. Although the results in this study are from creep failure tests under constant humidity and temperature condition, the relation seems to hold even under cyclic humidity conditions [8, 35].

The underlying mechanism of such relation is obviously damage evolution during creep, by which both lifetime and secondary creep rate are affected. It is, therefore, very interesting to prove this empirical relation from a fundamental damage evolution mechanism. Although many researchers attempted to use Monkman-Grant equation to "predict" lifetime, it should be noted that measuring secondary creep rate is equally time-consuming and equally variable as creep lifetime [1]. Secondly, the relation obviously doesn't tell the variability itself, which is most important in end-use.

Comparison of the key parameters c, ρ, and β between kraft liner and test liner

In Table 1, a summary of the key parameters for the two linerboards are shown.

As expected, the compressive strength of the kraft liner was higher than that for the test liner. For the uniformity parameter β, the difference between kraft liner

Table 1. A summary of the key parameters for a bleached kraft liner and an unbleached test liner.

	Compressive strength(N) (10 mm/min displacement rate)	*Uniformity parameter (β) (Averaged over different loads)*	*Load sensitivity parameter (ρ)*	*Parameter c*
Bleached Kraft liner	43.8 (42.4–45.3)*	0.49 (**)	53.5 (***)	1.64×10^{-44} (***)
Unbleached Test liner	39.0 (38.3–39.7)*	0.54 (**)	47.7 (***)	3.04×10^{-42} (***)

*: Upper and lower bounds of 95% confidence interval. **: The confidence intervals are shown in Fig. 9. ***: The confidence intervals were not available because of the lack of sufficient degree of freedom

and test liner was rather small, as seen also in Fig. 9. It was also true for the load sensitivity parameter: the value for the kraft liner is in the same range as those for the test liner. As expected from Eq. (12), the parameter c is very much the reflection of compressive strength: the higher the compressive strength, the lower the parameter c.

Therefore, within these two samples, there was no distinct difference in the characteristic parameters, except the parameter c. However, one should not extend this observation to a wider class of samples at this stage. Preliminary results showed that some pulping method does change the parameter ρ, so that the long-term behaviour is different from what is expected from the short-term property (compressive strength). As for the uniformity parameter β, there is no pre-existing information. It is, therefore, most interesting to re-examine the traditional pulping, papermaking, and converting effects on this parameter, as well.

CONCLUSION

Corrugated boxes and component boards have been designed based on static strength. As the demands for resource-efficient packaging continue, board manufacturers and box producers are facing increasingly difficult challenges of reducing weight (light-weighting), reducing cost, and increasing strength. However, the new formulation presented in this paper indicates that the (average) strength is not the sole factor, but there are other important aspects of the board properties that control real end-use performance. These are represented by the three parameters: the parameter c that is related to the conventional strength *and* its uniformity, the parameter ρ that is related to durability or endurance, and the parameter β the uniformity/reliability of the long-term response (creep lifetime). These have been determined experimentally in this study. Anecdotes have been accumulated in the fields that it is feasible to develop high performance by reducing variability of both long-term and short-term responses. The next step of our studies is, therefore, to examine pulping, papermaking and converting effects on these key parameters, together with the development of a more efficient method for determining the parameters.

The creep data reported in this article is still part of the long-term fundamental study of the authors' group for establishing load-scaling law and damage evolution law in the model. Further creep tests are planned at lower levels of load and under controlled humidity histories, and the results will be reported subsequently.

ACKNOWLEDGEMENTS

The authors would like to thank financial supports of Bo Rydin foundation. The authors also thank SCA (R&D, Obbola mill, and Munksund mill), and Billerud, Gruvön mill for providing samples and for giving valuable insights from technical discussions. The authors also would like to thank Professor Bo Westerlind for his various helps and suggestions made to this project.

REFERENCES

1. Coffin, D., *Creep and relaxation*, in *Engineering Mechanics of Paper and Board Products*, K. Niskanen, Editor. 2011, De Gruyter: Berlin. p. 111–137.
2. Considine, J.M., D.L. Stoker, T.L. Laufenberg, and J.W. Evens, *Compressive creep behaviour of corrugating components affected by humid environment*. TAPPI Journal-Technical Association of the Pulp and Paper Industry, 1994. **77**(1): p. 87–96.
3. Koning, J.W. and R.K. Stern, *Long-term creep in corrugated fibreboard containers*. Tappi, 1977. **60**(12): p. 128–131.
4. Moody, R.C., *How dead load, downward creep influence corrugated box design*. Packaging Engineering, 1966. **11**(8): p. 75–81.
5. Morgan, D.G. *Analysis of creep failure of corrugated board in changing or cyclic humidity regimes*. in *59 Appita Annual Conference and Exhibition*. 2005. Auckland, New Zealand: Appita.
6. Nyman, U., *Continuum Mechanics Modelling of Corrugated Board*, in *Dept. Structural Mechanics*. 2004, Lund University: Lund.
7. Popil, R.E. and B. Hojjatie, *Effects of component properties and orientation on corrugated container endurance*. Packaging Technology and Science, 2010. **23**(4): p. 189–202.
8. Popil, R.E. and M.K. Schaepe. *Dependence of corrugated container lifetime on component properties*. in *Progress in Paper Physics Seminar*. 2008. Espoo, Finland: TKK (Helsinki University of Technology).

9. Uesaka, T., *Statistical aspects of failure of paper and board*, in *Engineering Mechanics of Paper and Board Products*, K. Niskanen, Editor. 2011, De Gruyter: Berlin.
10. Uesaka, T. and J. Juntunen, *Time-dependent, stochastic failure of paper and box*. Nordic Pulp and Paper Research Journal, 2012. **28**(2): p. 370–374.
11. Coleman, B., *On the strength of classical fibres and fibre bundles*. Journal of the Mechanics and Physics of Solids, 1958. **7**(1): p. 60–70.
12. Coleman, B.D., *Time dependence of mechanical breakdown phenomena*. Journal of applied physics, 1956. **27**(8): p. 862–866.
13. Coleman, B.D., *Time dependence of mechanical breakdown in bundles of fibres. I. Constant total load*. Journal of applied physics, 1957. **28**(9): p. 1058–1064.
14. Coleman, B.D., *Statistics and Time Dependence of Mechanical Breakdown in Fibres*. J. Applied Physics, 1958. **29**(6): p. 968–983.
15. Alfthan, J., *The effect of humidity cycle amplitude on accelerated tensile creep of paper*. Mechanics of Time-Dependent Materials, 2004. **8**(4): p. 289–302.
16. Coffin, D. and C.C. Habeger, *The practical influence of heterogeneity on tensile accelerated creep in paper*. Tappi Journal, 2001. **84**(3).
17. Habeger, C. and D. Coffin, *The role of stress concentrations in accelerated creep and sorption-induced physical aging*. Journal of Pulp and Paper Science, 2000. **26**(4): p. 145–157.
18. Habeger, C., D. Coffin, and B. Hojjatie, *Influence of humidity cycling parameters on the moisture-accelerated creep of polymeric fibres*. Journal of Polymer Science Part B: Polymer Physics, 2001. **39**(17): p. 2048–2062.
19. Padanyi, Z. *Mechano-sorptive effects and accelerated creep in paper*. in *1991 International Paper Physics Conference*. 1991.
20. Curtin, W. and H. Scher, *Algebraic scaling of material strength*. Physical Review B, 1992. **45**(6): p. 2620.
21. Curtin, W.A. and H. Scher, *Analytic model for scaling of breakdown*. Physical Review Letter, 1991. **67**(18): p. 2457–2460.
22. Duxbury, P.M. and P.L. Leath, *Exactly solvable models of material breakdown*. Phys. Rev. B, 1994. **49**(18): p. 12 676–12 687.
23. Hansen, A., E.L. Hinrichsen, and S. Roux, *Scale-invariant disorder in fracture and related breakdown phenomena*. Physical Review B, 1991. **43**(1): p. 665–678.
24. Harlow, D.G. and S.L. Phoenix, *The chain-of-bundles probability model for the strength of fibrous materials I: Analysis and conjectures*. J. Composite Materials, 1978. **12**(April): p. 195–214.
25. Harlow, D.G. and S.L. Phoenix, *Bounds on the probability of failure of composite materials*. International Journal of Fracture, 1979. **15**(4): p. 321–336.
26. Phoenix, S.L., *Stochastic strength and fatigue of fibre bundle*. International Journal of Fracture, 1978. **14**(3): p. 327–344.
27. Phoenix, S.L. and R. Raj, *Scalings in fracture probabilities for a brittle matrix fibre composite*. Acta Metall. Mater., 1992. **40**(11): p. 2813–2828.
28. Phoenix, S.L. and L. Tierney, *A statistical model for the time dependent failure of unidirectional composite materials under local elastic load-sharing among fibres*. Engineering Fracture Mechanics, 1983. **18**(1): p. 193–215.

29. Tierney, L., *Asymptotic bounds on the time to fatigue failure of bundles of fibres under local load sharing*. Advances in Applied Probability, 1982: p. 95–121.
30. Hristopulos, D. and T. Uesaka, *Structural disorder effects on the tensile strength distribution of heterogeneous brittle materials with emphasis on fibre networks*. Physical Review B, 2004. **70**(064108): p. 1–18.
31. Alava, M.J., P.K.V.V. Nukala, and S. Zapperi, *Statistical models of fracture*. Advances in Physics, 2006. **55**(3–4): p. 349–476.
32. Uesaka, T., *Principal factors controlling web breaks in pressrooms – Quantitative evaluation*. Appita Journal, 2005. **58**(6): p. 425–432.
33. Stott, R.A., *Compression and stacking strength of corrugated fibreboard containers*. Appita, 1959. **13**(2): p. 84–89.
34. Fellers, C., *The significance of structure on the compressive behaviours of paper*, in *Paper Technology*. 1980, Royal Institute of Technology: Stockholm.
35. Bronkhorst, C.A., *Towards a more mechanistic understanding of corrugated container creep deformation behaviour*. J. Pulp and Paper Sci., 1997. **23**(4): p. J174–J180.
36. Urbanik, T., *A more mechanistic model of the compression strain-load response of paper*. Journal of Pulp and Paper Science, 2002. **28**(6): p. 211–216.
37. Monkman, F.C. and N.J. Grant. *An empirical relationship between rupture life and minimum creep rate in creep-rupture tests*. in *proc. ASTM*. 1956.
38. Urbanik, T.J. and B. Frank, *Box compression analysis of world-wide data spanning 46 years*. Wood and fiber science, 2006. **38**(3): p. 399–416.
39. Frank, B., *Corrugated box compression – A literature survey*. Packaging Technology and Science, 2013.
40. Billerud, *CCT10 defines true performance: The test method that reduces waste*: Solna, Sweden.
41. Kellicutt, K.Q. and E.F. Landt, *Safe stacking life of corrugated boxes*. Fibre Containers, 1951. **36**(9): p. 28–38.
42. Pierce, F., *Tensile tests for cotton yarns*. Journal of Textile Industry, 1926. **17**: p. 355.
43. Weibull, W., *A statistical theory of the strength of matertials*. Vol. 151. 1939, Stockholm, Sweden: The Royal Swedish Institute for Engineering Research.

APPENDIX

Following is the procedure to determine the key parameters in the Coleman's equation (Eq. (5)). This procedure is also known as Weibull plot, and is an effective way of examining whether the data fit to Weibull distribution or not. Let's restate Eq. (5) as follows.

$$F(t_B) = 1 - exp\{-cf_0^{\rho\beta} t_B^{\beta}\} \tag{A-1}$$

The above equation can be transformed by simple algebra into Eq. (A-5) as follows:

$$\boldsymbol{1 - F(t_B) = exp\{-cf_0^{\rho\beta} t_B^{\beta}\}} \tag{A-2}$$

$$\boldsymbol{log\big(1 - F(t_B)\big) = log\big(exp\{-cf_0^{\rho\beta} t_B^{\beta}\}\big)} \tag{A-3}$$

$$\boldsymbol{log\big(1 - F(t_B)\big) = -cf_0^{\rho\beta} t_B^{\beta}} \tag{A-4}$$

$$\boldsymbol{log\left(-log\big(1 - F(t_B)\big)\right) = log c + \rho\beta \cdot log f_0 + \beta \cdot log t_B} \tag{A-5}$$

Equation (A-5) indicates that by plotting the left-hand side of Eq. (A-5) against log t_B in the right-hand side, we have a linear relation between them, such as shown in Fig. A-1, *provided that Weibull distribution holds*. This is actually the way to check if the data follow Weibull distribution. The slope of this line, β, represents Weibull exponent (or Weibull shape factor), a measure of the uniformity of the distribution, as we will see shortly. Other parameters can be determined in a similar way. For example, suppose the distribution is measured for different load levels f_0. By plotting the intercept (the first and second terms in Eq. (A-5)) against log f_0, we obtain the slope ρβ and the intercept log c. From these equations, we can, therefore, determine all parameters, c, ρ, and β.

As seen in Eq. (A-5), the effects of load (the second term) and sample size (the first term, not explicitly shown) are all included in the intercept of the Weibull plot. This means that these effects appear as a vertical shift in the Weibull plot, such as illustrated in Fig. A-1.

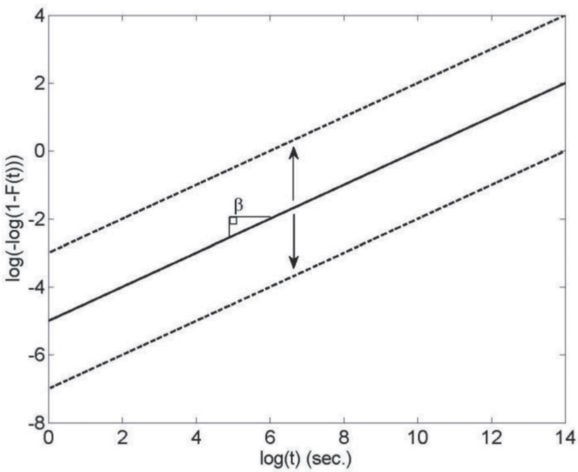

Figure A-1. Weibull plot.

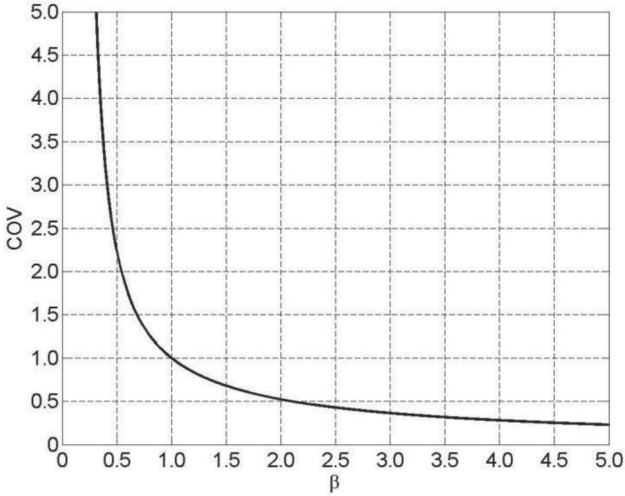

Figure A-2. COV as a function of Weibull exponent (β).

Because of this special plotting form, Weibull plot tends to emphasise tail distributions. Therefore, small scatters of the data in low tail tend to be magnified when plotted in this form.

Another important information on Weibull exponent (β) is that it is uniquely related to a more familiar statistical parameter, namely coefficient of variation (COV) (Eq. (8)). Figure A-2 shows the relationship between COV and Weibull exponent (β). As β decreases, the COV increases rapidly, particularly at $\beta \ll 1$. The higher the β, the lower the COV, that is, the more uniform the distribution is. This is why it is also called the uniformity parameter.

Transcription of Discussion

TIME-DEPENDENT, STATISTICAL FAILURE OF PAPERBOARD IN COMPRESSION

Amanda Mattsson and *Tetsu Uesaka*

Mid Sweden University, FSCN, Sundsvall, Sweden

Jean-Claude Roux Grenoble Institute of Technology-Pagora

Very interesting talk. I have one question and comment. You used a method which can be very dangerous, in order to determine your three parameters. I will explain. You used an elegant method involving the logarithm of a logarithm. In fact, from a mathematical point of view, the log can reduce variability of the data, and if you use it once again, you reduce again the variability of the data. So my question is, have you tried to find another method, I mean some minimisation of a function, in order to be much more confident with the parameters you would like to study and analyse?

Amanda Mattsson

Yes, that's a good question. No I have not tried any other way to determine these parameters yet. In fact, taking log twice actually magnifies the spread in low tail, rather than decreasing it. As I mentioned, we are now in the phase of trying to develop a quicker way of doing this. This will be done by standard compression tests at different loading rates.

Doug Coffin Miami University

Thank you, that was a very nice presentation and I understand, fairly well, everything you have done. The one question that still remains in my mind is this: if we consider your test on the paper, you did the tensile (compressive) test on the same size sample as the creep test and there is no scaling length difference? So that the scaling part of Coleman's theory does not apply to the statistics, if you compare the statistics of the tensile test to the statistics of the creep test? When I think about the compression strength test distribution, it follows Weibull with a high *K* because of the nonlinearity in the creep with load dependence. If I looked at the distribution of the log of lifetime, what I would see resembles Weibull with the high *K* value. If I look at probability versus log lifetime, I am sure we will never begin with zero lifetime because I cannot have less than zero lifetime. So I shove the distribution up against zero and it makes it look like *K* is less than 1, but as I reduce to really low load, I would expect to have that Weibull with the high *K*. In effect, the *K* would change with load level. I understand it probably makes little practical difference which way you go, but fundamentally, I want to understand the difference in constant *K* versus load dependent *K*.

Amanda Mattsson

Yes, we discussed this yesterday. Here we are looking at this probability density function (figure 8). If we have a very-very low load, but the plot is actually normalised, then we obtain figure 8. But if it is not normalised, we will find something like this: we will have very, very small probability of failure along the whole x-axis.

Doug Coffin

So I take that curve and, instead of plotting versus lifetime, I plot versus log lifetime. To me, at low load levels, it would just look like the strength distribution and, as I go down in load, I would shift that distribution to longer lifetime versus always keeping it peaking at zero. My thought is that the log of lifetime distribution would look the same as the strength distribution, but maybe shifted a little bit; as I decrease load, I would just be shifting it on the log axis, not closing it in. That is the difference that I would like you to think about.

Warren Batchelor Monash University (from the chair)

You said that you were trying to speed up the measurement process but by how much? We have got two samples here, how long did actually measuring all of the data take?

Amanda Mattsson

So far, it has taken approximately one year to accumulate these data points, so it would be good to speed it up a little. We are actually in the phase of determining these parameters by performing strength measurements with different loading rates. So, hopefully, we will obtain the same parameter estimates as we did with the creep tests. The creep tests are performed in order to validate how well the model describes the actual behaviour.

Sören Östlund KTH

I just need to ask about the equations driving the rate of damage development. Consider equations (1) and (2). You say that equation (2) is only a function of time, which means that you implicitly say that the damage development is not a function of damage. Can you comment on that? I mean if you have more damage to the fibre then the damage development rate might increase, but you do not have damage inside the damage evolution function. It is very important in the rest of the equation, but it is interesting how you motivate this assumption in equation (2) based on the general expression in Equation (1).

Amanda Mattsson

Yes, some explanation is missing in between the two equations. It has been shown in the literature that this form of the evolution equation holds widely.

Sören Östlund

But you assume that damage development is not dependent on how much damage you have?

Amanda Mattsson

No, exactly.

Tetsu Uesaka Mid Sweden University (co-author)

Certainly, in the damage mechanics area which is very much established in the solid mechanics area, you obviously have omega as a parameter in the evolution equation, but it depends on the kind of cross-sectional area where degradation occurs and that is one of the damage models (e.g. Katchanov's model). But in this case, particularly in this fibre-based material, we are talking about very dispersed, scattered damage evolution, so it is very difficult to define such a geometric model at this stage. So, we have left it in the general form of Coleman's model. Secondly, to answer the question about the estimation of some of the key parameters: this Weibull plot has been used for many-many years in this area and certainly there is an issue of estimation, as you said. (Actually the issue is not suppressing the variation, but over-emphasising the scatter of low tail.) Accordingly, we are looking at some other methods such as the Maximum Entropy method. It is certainly something that will be done during the next stage of this investigation.